Ultrasound-Triggered Release from Micelles

[1]William G. Pitt

[1]Brigham Young University, Provo, UT, USA

[2]Ghaleb A. Husseini

[2]Laura N. Kherbeck

[2]American University of Sharjah, Sharjah, UAE

Corresponding Author: Dr. William G. Pitt

Chemical Engineering Department

Brigham Young University

Provo, UT 84602 USA

pitt@byu.edu

This is a preprint manuscript of:

Pitt, W. G., Husseini, G. A., & Kherbeck, L. N. (2013). Ultrasound-triggered release from micelles. In Alvarez-Lorenzo, C. & Concheiro, A. (Eds.), Smart materials for drug delivery, Vol.1, (pp. 148-178). The Royal Society of Chemistry, https://doi.org/10.1039/9781849736800-00148.

Table of Contents

6.4 The Future of Ultrasound-Triggered Drug Delivery from Micelles

6.5 References

6.0 Abstract

Ultrasound is an ideal trigger for site-actuated drug delivery because it can be focused through the skin to internal targets without surgery. Ultrasound can deposit thermal or mechanical energy through tissue heating or bubble cavitation respectively. Bubble cavitation can concentrate energy that can trigger drug release from carriers. Micelles are nanosized molecular assemblies of amphiphilic molecules that spontaneously form in aqueous solution and possess a hydrophobic core that can sequester hydrophobic drugs. This chapter reviews the literature regarding the use of ultrasound to release drugs from micellar carriers and provides a thorough analysis of the advantages and disadvantages of these nanovehicles. These carriers are composed of block copolymers, usually with polyethylene oxide blocks at the surface of the micelle. Release from polymeric micelles has been observed *in vitro* and *in vivo*. Tumors have been successfully treated using low frequency ultrasound and chemotherapeutics in polymeric micelles. The mechanisms of drug release are discussed. The prevalent theory is that gas bubble cavitation events create high shear stress and shock waves that transiently perturb the structure of the micelles and allow drug to escape from the hydrophobic core.

6.1 Introduction

The concept of triggered drug release is that some mild stimulus, a stimulus that is not harmful to healthy tissues and one that exists only in desired locations or that can be controlled in time and/or space, is required to permeabilize an otherwise impermeable vesicle carrying therapeutics. Ultrasound is such an ideal trigger. Ultrasound does not interact strongly with tissues, and when used appropriately at low intensities, there is no tissue heating or other damage. Ultrasound can be focused from an external device, through the skin and tissue, to the desired target site. There is no scalpel, blood or pain associated with delivery of ultrasound. The delivery of ultrasound can be electronically controlled in time, from a tiny pulse of high intensity, to a series of short pulses in rapid succession over seconds, to continuous low intensity application for minutes to hours. When compared to other external triggers such as radio frequency (RF) heating and magnetic fields, the temporal and spatial control of high frequency ultrasound cannot be surpassed. Only focused light can compete in these areas, and the high absorption and scattering of visible light limits its controlled application to relatively short penetrations depths into the body. While near infrared light can penetrate further than visible light, scattering is still a drawback. By comparison, low frequency ultrasound can penetrate centimeters into the body with very low scattering. In this aspect it is ideal.

As the complementary partner to complete this excellent controlled delivery system, a vehicle is required that can securely sequester the drug and then release it upon application of the ultrasound. For many drugs, a micelle is an ideal match in this partnership.

This chapter reviews the literature regarding the controlled release of therapeutics from micellar carriers using ultrasound (US) as a triggering mechanism. In addition to US, there are other types of external triggering mechanisms mentioned above,[1-3] and several types of passive

internal triggering mechanism, such as local pH,[4, 5] heat,[6] or local biochemistry.[7] We invite the interested reader to consider those stimuli, especially when comparing the advantages and disadvantages of ultrasound-triggered drug release from micelles.

This chapter begins with a description of ultrasound and micelles, then continues with a brief review of conventional micellar drug delivery, and finishes with a thorough review of ultrasonically triggered delivery from micelles and a discussion of the physical mechanisms involved.

6.2 Ultrasound

6.2.1 Physics of Ultrasound

6.2.1.1 Wave Nature of Ultrasound

Ultrasound (US) is simply high frequency pressure waves, just as audio sound is low frequency pressure waves. Physicists define US as pressure waves with a frequency of 20 kHz or higher, which is above the common threshold of hearing for humans.[8] As with sound and light waves, ultrasonic waves can be focused on a particular volume that has dimensions as small as about ½ the wavelength. The speed of sound in water and most tissue is about 1.5 km/s, so the wavelength of 1 MHz US is about 1.5 mm. Thus high frequency US (> 1 MHz) can be focused to fairly small volumes, which is useful for triggering release at precise locations in the body. However, low frequency US (20 kHz to 200 kHz) is more challenging to focus, not only because the spot size is larger, but the physical size of the transducer is also much larger if focusing is required. For example, the wavelength of 20 kHz US in water is about 7.5 cm, so focal spots cannot be much smaller than 4 cm in diameter, and a decent transducer that can focus adequately would be at least 15 cm in diameter. If the decision of which frequency to use were

based on focal volume size, one would select high frequency US for drug delivery applications. However, high frequency US has its own challenges.

The first challenge is the attenuation of the ultrasonic intensity by tissues in the body. This attenuation occurs by both scattering and absorption.[9] Each tissue has its unique attenuation and speed of sound, which have been tabulated.[10, 11] The challenge arises because high frequency US is attenuated more than low frequency US, and the attenuation increases fairly proportionally to frequency in tissue.[9, 12] Thus, although high frequency US can be focused nicely, its high absorption prevents its penetration deeply into the body, and scattering reduces some of the focal precision endowed by the high frequency. Because the attenuation increases with frequency, the depth of penetration into body tissue is 10 times shorter at 2 MHz than at 200 kHz. High frequencies above 5 MHz simply do not penetrate sufficiently to deliver high energy densities without the concomitant heating of the tissue (see section 6.2.1.2).

In comparison, low frequency US is easily propagated through all tissues except bone and lung, and thus is easily delivered to all tissues except lung, bone, marrow, and brain. As mentioned, however, the spatial focusing is more problematic. There are advanced techniques that, by using interference between multiple transducers, can create local volumes of focused ultrasound. These techniques are not yet common and are outside of the scope of this review, but they may have important future applications in volume-controlled drug delivery using low frequency US.

The second main challenge facing high frequency US is that the key mechanism usually employed as a trigger for ultrasonic drug delivery, called gas bubble cavitation, is much more effective at lower frequencies as will be discussed in section 6.2.1.3. Thus for drug delivery from

a micelle, which usually requires deep tissue penetration and active gas bubble cavitation, low frequency US is much more practical and is often used in the research lab.

6.2.1.2 Ultrasonic Heating

What happens to all of the attenuated energy of high frequency US? It is converted into heat. Thus ultrasonic heating of tissues increases proportionally to the frequency. Imaging ultrasound employs high frequencies, but only in very short pulses, and thus the average amount of heat deposited in the tissues is low. Nevertheless, there are safety considerations employed to prevent the thermal damage of tissue during diagnostic ultrasonic exposure. The safety level is usually expressed by the Thermal Index (TI), which is the ratio of the applied acoustic power to the power required to raise tissue temperature by 1°C. For example, an exposure with a TI of 1 would raise tissue temperature by 1°C and a TI of 3 would raise the temperature by 3°C. Most diagnostic ultrasound imaging equipment calculates and displays the TI on the screen so as to avoid overheating.

Since the TI is proportional to the heating, as the frequency increases, the TI also increases. For an equivalent exposure intensity (same power density, pulse frequency, pulse length, etc.), there would be much more heating at 1 MHz than at 100 kHz. Again consideration of this parameter points to the advantage of lower frequency ultrasound allowing higher intensities and longer durations of exposure.

6.2.1.3 Mechanical Cavitation

Cavitation is the formation and dynamic oscillation of gas bubbles in a liquid and is a very common and significant phenomenon when ultrasound is applied in any aqueous environment. The oscillating pressure wave causes gas bubbles to expand (as pressure decreases) and contract (as pressure increases) in a cyclic manner. This mechanical movement of the bubble and the

surrounding fluid interface creates stresses on nearby cells and vesicles (such as micelles) and causes flow of fluid and movement of particles. Cavitation is generally divided in two general categories – stable and inertial – depending upon the amplitude and nature of the bubble oscillation.

Stable cavitation, also called non-inertial cavitation, occurs at relatively low amplitude pressure oscillations and when the frequency of the oscillation does not match the natural resonance frequency of the bubble. In stable cavitation the bubble usually undergoes many repetitive cycles of expansion and contraction without any chaotic behavior. Although there is no violent collapse as is the case with inertial cavitation, the oscillations create fluid flow adjacent to the bubble, called microstreaming.[12, 13] Very near the surface of the bubble the fluid velocity gradients are very high, creating strong local shear stress.[14-16] Stable cavitation is usually detected by listening with a hydrophone to the pressure waves emitted from bubbles as they oscillate. At very low amplitudes, the only oscillations are those matching the frequency of US applied to the bubbles. But as the amplitude increases, non-linear oscillations are formed which produce emissions at higher harmonics ($2f$, $3f$, $4f$, etc.) of the applied ultrasonic frequency f.[12, 13, 17] As the amplitude increases further, subharmonics ($f/2$, $f/3$, etc.) and ultraharmonics ($3f/2$, $5f/2$, $7f/2$, etc.) appear. Although the cavitation may remain stable, the appearance of subharmonics usually indicates that the bubbles are near the transition to chaotic behavior associated with collapse cavitation.

Collapse cavitation occurs at relatively large pressure amplitudes or when the resonance frequency of the bubble is near the ultrasonic frequency. It is characterized by large amplitude chaotic (non-repetitive) oscillations that quickly lead to the "collapse" of the gas bubble that occurs when the momentum of the inward moving spherical wall of water is so great that the

opposing pressure from the compressed bubble cannot stop the water from compressing the gas to a super-critical fluid. The temperatures and pressures calculated in such a collapse exceed 5000 K[18, 19] and 100 atm.[13] These high temperatures cause dissociation of water and gas molecules into free radicals that can be captured as evidence of and quantification of collapse cavitation.[20-23] The collapsing walls can attain or exceed the speed of sound in air (~340 m/s), creating a spherical shock wave inside the bubble that slams in on itself and then rebounds as a spherical pressure shock wave emanating outward from the site of bubble collapse. The expansion of the supercritical fluid back into gas creates an outward expanding gas bubble. If for some reason the inward collapse or outward expansion is not spherically symmetrical, the bubble will be fragmented into smaller bubbles that will start to grow and cavitate also. Because the inertia of the water (as opposed to the pressure in the bubble) dominates the behavior of these oscillations, this type of cavitation is often called "inertial cavitation". In the past this has been called collapse cavitation and transient cavitation because the bubble existed only transiently before it was "destroyed" by fragmentation.

Needless to say, collapse cavitation is a very violent event, particularly in the near vicinity of the collapse event. The high fluid shear stresses associated with the sudden collapse and rebound of the bubble are thought to be sufficient to damage cell membranes, disrupt liposomes and shear micelles, as illustrated in Figure 1. The shock wave can produce compressive and shear stresses in membranes. Free radicals can react with other molecules or with biomolecules in the cells with toxic results. Collapse cavitation has been correlated with drug release from liposomes[24, 25] and from micelles.[26, 27] Collapse cavitation in blood vessels can denude the surface of endothelial cells,[28] permeabilize capillaries[29, 30] and even breach the blood-brain barrier.[31-35] Despite these seemingly negative consequences, collapse cavitation does have some positive

aspects. Vigorous fluid flow in the region of cavitation enhances the local convective transport of drugs. Also, carefully controlled cavitation is used to transiently open cell membranes (called sonoporation) for gene delivery,[36] for careful breaching of the blood-brain barriers,[31, 33] for purposeful destruction of tumors or other unwanted lesions or tissues,[37] and for disruption of blood clots.[38-41]

The extent of collapse cavitation can be characterized by measuring the production of free radicals[20, 21] and by examining the acoustic emissions.[39, 42, 43] When listening with a hydrophone, the onset of collapse cavitation is characterized by a sudden increase in the baseline of the acoustic spectrum. The harmonics, subharmonics and ultraharmonics are still present, but they sit on top of a much higher baseline of noise that suddenly appears because of the "white noise" produced in the frequency spectrum by the generation of shock waves.

One of the principal questions in bubble cavitation regards the onset of collapse cavitation. A general observation was that for a given acoustic pressure amplitude, cavitation occurred more readily at lower frequencies. To validate this observation, computer simulations were done to calculate when air bubbles of various sizes would experience inertial cavitation in blood and water.[44] The data showed that the threshold for onset of inertial cavitation in a field of bubbles with a spectrum of sizes was proportional to the amplitude of the negative pressure cycle (peak negative pressure, p^-), and inversely proportional to the square root of the ultrasonic frequency, f. This supported the observation that as frequency decreased, the inertial cavitation increased. These observations led to the definition of the "Mechanical Index", $\mathbf{MI} = p^- / \sqrt{f}$, where p^- is in MPa and f is in MHz. Along with the Thermal Index, TI, the MI is displayed on most ultrasonic imaging machines, and there are guidelines as to the maximum MI value for safely imaging

various tissues, such as fetal tissue, eyes, heart, etc.[45, 46] The original purpose of MI was to avoid damaging delicate tissues with collapse cavitation events, but the MI can also be used as an indicator of the amount or intensity of collapse cavitation that might be expected if bubbles are already present.

The MI concept was developed for a general distribution of bubbles with a range of sizes, assuming that at least one of those bubbles would have a resonance frequency near the applied frequency. If, however, there is only one bubble size and the objective was to cause collapse cavitation, then it would be important to select the frequency based on the bubble size. Although more rigorous equations are available,[13] a simplified relationship between the resting bubble radius (R_0, radius with no applied pressure) and the resonance frequency, f_{res}, is given by[46] $f_{res} = 3.3 m/s / R_0$. This indicates that a small bubble with a radius of about 1 μm has a resonance frequency of 3.3 MHz. Such small bubbles are used as contrast agents in medical imaging, and imaging instruments operating at about 3.3 MHz would tend to create collapse cavitation, even at low amplitudes.

There are a few other interesting cavitation phenomena that pertain to drug delivery from micelles. The first is the generation of "micro jets" from the collapse of a bubble near a solid surface. The presence of the surface reduces the inward flow of liquid from that direction, resulting in an asymmetric collapse of the bubble in a manner that creates a high velocity jet of liquid shooting directly at the surface.[12, 13] A cell has a sufficiently viscous surface that cavitation near a cell has been observed to shoot a micro jet toward the cell and pierce the cell membrane.[47] It is believed that this mechanism is responsible for the "sonoporation" phenomenon used for ultrasonic gene delivery.[36, 47]

A second phenomenon called "acoustic pressure" is caused by the pressure waves emanating from an oscillating bubble.[17, 46] The oscillations generate a net force on other objects in the vicinity of the bubble. If the object is denser that the surrounding liquid, the net force is directed toward the bubble, whereas a less dense object feels a force directed away from a bubble. These forces have been observed experimentally.[48] This acoustic pressure is very useful for drug delivery from micelles. In a mixture of bubbles and micelles, the bubbles, which are less dense than water, will push themselves away from each other and spread out. The micelles, which are denser than water, will be pulled toward the nearest bubble. At very short distances the fluid shear rates can approach 10^7 sec^{-1},[16] and these might be sufficient to disrupt the micelle structure.

So far in this discussion of cavitation, the bubbles were assumed to already exist. This is the case when specially engineered bubbles, usually stabilized with a shell of surfactant or protein, are introduced. A common source for these bubbles is the "contrast agent" used in diagnostic sonography. These bubbles are usually from 1 to 5 μm in diameter, so they can be injected into the circulatory system. However the size of these bubbles prevents them from passing from the capillaries into the tissues. Smaller bubbles designed for drug and gene delivery are in development.[49] The existence of bubbles for drug and gene delivery in the extra-capillary space is a desirable research objective, but is difficult to attain.[50] However, new techniques involving the ultrasonic expansion of perfluorocarbon nanoemulsion droplets are being explored.[51-54]

Even in the absence of purposefully introduced bubbles, cavitation can still occur. Most fluids contain dissolved gases, such as oxygen and nitrogen from contact with air. Upon exposure to ultrasound, the negative pressure fluctuations can cause dissolved gasses to nucleate into bubbles that may persist, particularly if they can be stabilized by a layer of surfactants.[13] Such surfactants can be proteins in the blood or extra-capillary space. Thus it is possible to

generate bubbles and then cavitate them *in vitro* or *in vivo*, even in the absence of contrast agents. However, the acoustic intensities required to form bubbles are generally so high that once formed, the bubbles grow by diffusion of more dissolved gas, and then quickly undergo collapse cavitation, fragment into smaller bubbles, grow again, and continue the cycle.[12, 13] Thus vigorous collapse cavitation can occur even when contrast agents or other bubbles are not introduced. In extremely clean and degassed water, the likelihood of bubble formation is decreased.

6.2.1.4 Acoustic Streaming

Another mechanical effect, independent of the presence of bubbles is called "acoustic streaming". This occurs when the very small absorption of ultrasound by the water transfers the momentum from the absorbed sound to the fluid.[12, 13] This causes convective flow in the direction of the ultrasound wave propagation. Acoustic streaming happens to a greater extent in colloidal suspensions of cells and protein since these components absorb ultrasound better than pure water. Flows can move as fast as 10 cm/s,[55] but these flows do not have the extreme velocity gradients and shear stresses found in microstreaming and shock waves. The main beneficial effect of acoustic streaming is convective flow and mixing. There are reports of using acoustic streaming to press gas bubbles against blood vessel walls.[56]

6.2.1.5 Safety

The TI and MI safety indices described in 6.2.1.2 and 6.2.1.3 were developed in the 1990's to protect delicate tissues from damaging exposure to heat and cavitation stresses. These delicate tissues include the fetus, heart, eye and brain.[46, 57-60] In general there is less concern for thermal exposure and cavitation in other tissues because they have redundant architecture (kidneys, liver) or are non-essential (muscles, skin, etc.). There are also some reports of petechiae and thermal

damage to the skin at high levels of insonation.[61, 62] These problems were overcome by introducing different pulse sequences and cooling the transducers.[63, 64]

Another topic of concern is that insonation of a tumor with accompanying cavitation might release fragmented portions of the tumor into the circulatory system where they may lodge and grow in other tissues, creating a type of "induced metastasis". Studies designed to reveal ultrasonic enhancement of tumor metastasis found none, even with highly metastatic tumors.[65-67]

6.3 Micelles

6.3.1 Drug Delivery from Micelles

In the science of nanomedicine, one of the most useful carriers for efficient drug delivery is the micelle. Micelles are assemblies of amphiphilic molecules in spheres or rods with diameters ranging from 5 to 100 nm. In aqueous systems, the molecules arrange themselves with their hydrophobic groups toward the interior of the structure and the hydrophilic group toward the surrounding water. An advantage of micelles over other nanocarriers is their easy method of preparation, the simplicity of loading hydrophobic drugs into their core, their stability, and the fact that drug release from micelles can be controlled. Micelle stability is related to their critical micelle concentration (CMC), which is the molecular concentration below which the micelle will dissolve. A low CMC indicates that micelles will form readily and remain thermodynamically stable even in relatively low concentration. Once the micelles are diluted below their CMC, the rate of dissolution is related to the size of the amphipathic molecules. Micelles composed of

large polymeric molecules take longer time to disentangle and dissolve, and thus can persist in their metastable micelle form for minutes.[68, 69]

Micelles have been used in pharmaceutical applications for centuries because of their ability to absorb hydrophobic drugs into their core, thus increasing drug loading in traditional aqueous oral formulations. With the advent of technology to introduce micellar formulations directly into the circulatory system (via intravenous infusion), it was noted that some formulations suffered from rapid clearance due to their fast uptake by the cells the mononuclear phagocyte system (MPS). These micellar carriers persisted in circulation longer when coated with agents comprising poly(ethylene glycol) (PEG) .[70] The coating agents modified the surface of the colloidal drug carriers such that adsorption of opsonizing proteins was inhibited so that the cells of the MPS did not recognize and clear the carriers.[71] The ability of PEG-coated particles to inhibit adsorption of proteins depends on the surface density of PEO chains, their length and dynamics.[71] Prolonged circulation resulted in substantial increase of the area under the curve (AUC) of the blood concentration of the therapeutic agent over time.[72]

6.3.1.1 Traditional Surfactant Micelles

Before the advent of synthetic polymers, nearly all pharmaceutical formulations of micelles were composed of natural small surfactant molecules, such as fatty acids, alkyl esters of glycerol, phosphoglycerol esters and other amphiphilic molecules. It was found that the solubility of hydrophobic drugs could be greatly increased by adding these surfactants. These hydrophobic drugs were solubilized in the core of the micelle. The solubility of some amphiphilic drugs could also be increased by the addition of surfactants. These amphiphilic drugs partition to the interface between the hydrophobic core and the hydrophilic corona of the micelle.

With the progress of organic chemistry in the 20th century, the natural surfactants were supplemented by synthetic surfactants or semi-synthetic surfactants. These new additions broadened the scope of drugs that could be adequately solubilized for oral and intravenous delivery. Surfactants used in micelles are generalized in 4 categories: anionic (phosphates, carboxylates, sulfates, etc.); cationic (usually amine-containing surfactants); zwitterionic (phosphocholines and synthetic surfactants) and nonionic (ethoxylates, glucosides, and more).[73] The charge and chemistry of the hydrophilic head group has a large effect on the solubilization capacity and the CMC. In general, the nonionic surfactants have the greatest solubilization capacity, the anionic surfactants have the least, and cationic and zwitterionic surfactants fall in between.

While some surfactant micelles have very low CMC values, polymeric micelles have even lower CMC values.[74] Once the concentration drops below the CMC, surfactant micelles usually dissolve faster than polymeric micelles. Therefore there is a trend to move towards polymeric micelles in new pharmaceutical formulations. To our knowledge there are no reports of ultrasonic-activated drug delivery from traditional non-polymeric micelles. However, that does not preclude the possibility of using surfactant micelles for ultrasonic drug delivery. Natural surfactants may have advantages in safety and biocompatibility.

6.3.1.2 Polymeric Micelles

It is attractive in drug delivery to use polymeric micelles comprised of hydrophobic-hydrophilic block copolymers, with the hydrophilic block containing PEG or other hydrophilic chains. These micelles usually have a spherical, core-like structure with the hydrophobic block forming the core and PEG chains forming the corona. Several types of these copolymers have

been proposed. Among them, AB-type block copolymers, such as poly(L-amino)-co-poly (ethylene oxide)[75-78] and ABA-type block copolymers, such as the Pluronics.[79-81]

Another class of these copolymers include poly(ethylene oxide-*b*-isoprene-*b*-ethylene oxide) triblock copolymer in which the isoprene blocks comprising the core were crosslinked by UV irradiation, rendering micelles stable in blood circulation.[82]

As mentioned above, a particularly popular and useful family of polymers for micellar drug delivery is the family of Pluronic polymers, triblock copolymers of poly(ethylene oxide) (PEO) – poly(propylene oxide) (PPO)- poly(ethylene oxide) (PEO). They are mostly water-soluble, and form micelles at various CMC values, depending on the ratio of PPO to PEO segments.[83] The hydrophobic block forms the core of the micelle and the hydrophilic PEO chains form the corona, resulting in a spherical core-shell structure.

Pluronic P105 is a particularly useful micelle-forming polymer because it easily dissolves in water and yet can carry a good payload of hydrophobic drugs.[84, 85] The disadvantage with Pluronic P105 micelles is the relatively high CMC, such that when it is diluted upon intravenous injection, its local concentration drops below the CMC and the micelles start to dissolve.[86] To overcome this problem, the micelles were stabilized by polymerizing an interpenetrating network (IPN) of poly(*N*,*N*-diethylacrylamide) (NNDEA).[87] NNDEA was dissolved into and then polymerized within the Pluronic P105 micelles, which resulted in an IPN that markedly slowed the dissolution of P105 chains from the micelle. Cross-linking the NNDEA network increased micellar stability such that the micelle could sequester hydrophobic molecules for weeks before total dissolution.[88]

Tests were conducted in order to determine whether such stabilization would affect the ability of the micelles to sequester and release the drug doxorubicin (Dox). It has been shown that the amount of drug released and its subsequent re-encapsulation were not very different from the behavior observed for unstabilized micelles, but had the added bonus of slow dissolution of the micelles. The stabilized micelles released the Dox by application of 70 kHz ultrasound, as will be discussed in section *6.3.2.1*.[89]

Pluronic copolymers at different aggregation states have been tested as drug carriers.[90-95] Pluronic molecules in the unimeric form (below the critical micelle concentration) were found to greatly enhance the cytotoxic activity of a wide variety of drugs. Above the critical micelle concentration, Pluronic molecules form dense micelles with a lipophilic core that encapsulate the drugs within that core.[96]

Pluronic and other amphiphilic copolymer micelles are recognized as some of the most novel types of carriers for chemotherapy drugs. The drug is usually introduced into the polymer matrix by mixing, and (in the absence of ultrasound) is slowly released upon the dissolution or degradation of the micelle or by drug diffusing from the micelle.[97] Of particular interest is poly (lactic acid)-b-poly(ethylene glycol) (PLA-b-PEG) since it is biodegradable, biocompatible, and exhibits proper hydrophilic/hydrophobic balance. Its degradation products are non-toxic and can be excreted by the kidneys.[91] Several methods of loading PLA micelles with the drug Dox have been investigated.[98] There are many variations on this structure that employ the hydrolysis of PLA to control drug release.[99-101]

Related to PLA are other polyesters, such as poly(ε-caprolactone) (PCL). For instance, a self-assembled PEG-PCL diblock copolymer micelle was designed to solvate and deliver the very

hydrophobic drug honokiol.[102] PCL micelles have received some recent attention as drug carriers.[103-105]

While polymeric micelles are sometimes praised for their high loading capacity for hydrophobic therapeutics[106], exceeding the maximum loading capacity may cause the drug to precipitate. Furthermore, the aggregation number of the copolymer was found to influence the drug loading efficiency of the micelle – a greater amount of drug can be incorporated into the core of a micelle with a higher aggregation number.[69]

6.3.1.3 Drug-Polymer Conjugates

Drug-polymer conjugates have been a rapidly developing field since they were first proposed in the mid 1970's, and nearly a dozen such carriers have now progressed to the clinical trial stage.[107] These include *N*-(2-hydroxypropyl) methacrylamide (HMPA)-Dox for lung and breast cancers,[108] HPMA-platinate for ovarian cancers and melanomas,[109] poly ethylene glycol (PEG)-poly(Aspartic acid) ASP+-Dox micelles for pancreatic cancer,[110] and most importantly poly(L-glutamic acid) (PG)-paclitaxel for breast, colorectal, ovarian, and lung cancers.[111, 112] The latter is in Phase III clinical trials and is on track to become the first drug-polymer conjugate to be used in hospitals.[113] To synthesize drug-polymer conjugates, the chemotherapeutic agents are covalently bonded to a water-soluble polymer. For example PG-TXL is covalently attached to PG via an ester bond utilizing the 2'-hydroxyl moiety using a dicyclohexylcarbodiimide (DCC).[111] NMR confirmed the desired conjugation and it was estimated that seven TXL molecules are bonded to each PG chain. The new drug polymer conjugate suppressed the growth of murine ovarian carcinoma tumors in all 26 mice used in the study. After 2 months, 96% of the mice remained histologically free of the ovarian carcinoma.[111]

In another study, Nakanishi et al succeeded in synthesizing a PEG-ASP-Dox conjugate. Since this drug delivery molecule has PEG on its outer surface, it was rendered stealthy and was able to circulate for longer periods of time without being recognized by the MPS.[110] Starting with PEG-NH_2 and the BLA-NCA (the unit of Aspartic Acid), the synthesis followed three steps: elongation and acetylation, debenzylation, and finally the partial conjugation to Dox. This carrier showed significant antitumor activities in five different tumor types when compared to free Dox administered in a PBS solution.

Active targeting is also possible with drug-polymer conjugates by attaching a targeting moiety to the polymer. The advantages of drug-polymer conjugates are similar to those of self-assembled micelles and, most importantly, drug-polymer conjugates help overcome multi-drug resistance (MDR). Next we will discuss different targeting techniques that include passive targeting, active targeting, and targeting using external stimulus.

6.3.2 Targeting

6.3.2.1 Passive Targeting

Blood vessels of healthy tissue have tight inter-endothelial junctions, while tumors often exhibit defective microvasculature with large inter-endothelial gaps. Those gaps result in heightened vascular permeability that allows sub-micron particles to extravasate beyond the capillaries. Passive targeting is based on the enhanced permeability and retention (EPR) effect that allows extravasation of drug-loaded nanoparticles through such defective microvasculature in tumors. Furthermore, tumors often exhibit poor lymphatic drainage, which reduces clearance of the extravasated carriers from the tumor tissue. Extravasation of nanoparticles does not occur in healthy tissue blood vessels except for specialized tissues such as the liver and kidneys. The

accumulation of nanoparticles by the EPR effect requires sufficient circulation time in blood for the particles to slowly collect in the tumor. As mentioned, coating nanoparticles with PEO chains increases circulation residence time and increases the amount of accumulation by the EPR effect.[114] Even so, usually less than 5% of the administered dose accumulates in the "targeted" tumor site by passive targeting means.[115]

There are many examples of passive targeting.[104, 116-124] For example, Shin et al. studied the delivery of several chemotherapeutic agents using a poly(ethylene glycol)-block-poly(lactic acid) (PEG-b-PLA).[116] These agents include poorly soluble anti-neoplastic agents including Paclitaxel (PTX), Etoposide (ETO), Docetaxel (DCTX), and 17-allylamino-17-demethyoxygeldanamycin (17-AAG). The study also characterized the loading and drug release profiles from micelles encapsulating 2- or 3- drug combinations. All loaded carriers had diameters in the range of 32-39 nm. Using turbidity measurements, 17-AAG was found to reduce drug precipitation, which in turn improves the stability of PEG-b-PLA micelles. Additionally, the study reported that single- and multi- drug micelles released their contents within 12 hours. The study concluded that this new formulation offers an effective method for administering chemotherapy agents with low solubility.

6.3.2.2 Active Targeting

There are some situations in which passive targeting is not sufficient, such as for targeting within the circulatory system or for more specific targeting once the particles have extravasated and there are both healthy and tumorous cells in the extra-capillary space. In this case it is

beneficial to attach small site-specific non-antigenic targeting ligands such as folic acid, antibodies, proteins (such as transferrin), sugars, or polypeptides.[125-128]

Tumor-specific targeting is possible when the tumor cells express some surface component that is not usually present on normal cells. For example a wide variety of human tumors overexpress folate-binding protein, a glycosylphosphatidylinositol-anchored cell surface receptor for the vitamin folic acid.[129] Another example is the overexpression of the human epidermal growth factor receptor II (HER2) complex on many cancer cells.[130]

Micelles can be directed to attach to these cells by conjugating the complementary ligand to the micelle. In many cases, the binding event will stimulate endocytosis of the ligand and its attached vesicle, thus introducing the therapeutic into the tumor, but still within an endosome. Subsequent escape from the endosome is required for maximal drug delivery. The number of ligands can be optimized to increase the efficacy of polymeric drug carriers.[131] Although the accumulation of micelles at the tumor site by passive targeting is largely independent of ligand attachment, ligand-conjugated micelles were found to demonstrate higher tumor fighting activity as compared to non-conjugated micelles, which is attributed to direct surface interactions.[132] Furthermore, these targeted carriers can be synthesized to respond to changes in pH, where drug release is accelerated in the intracellular acidic environments of endosomes and lysosomes (pH below 4.8).[132, 133]

One example of a folate targeted drug-polymer conjugate is the Dox-PLGA-PEG-FOL micelle, assembled by chemically conjugating Dox to the terminal end of PLGA in the diblock copolymer structure of PLGA-b-PEG and then separately conjugating folate to the terminal end of PEG.[134] Other examples of folated micelles include the amphiphilic block copolymers of methoxy poly(ethylene glycol) (MPEG) and poly(ε-caprolactone) (PCL)[135] and the chondroitin

sulfate-Pluronic® 127-folated nanogels, which are capable of inhibiting drug efflux transporters in chemotherapy.[136]

To synthesize folated Pluronic P105 micelles (P105-FA), 1,1-carbonyldiimidazole can be used. Such folated Pluronic micelles were able to release Dox using low frequency ultrasound.[136] Another study used cross-linked Pluronic micelles with folate conjugated to their surfaces as carriers of Dox and other anti-cancer drugs to target ovarian cancer. The study was conducted *in vivo* and significant anti-tumor effects have been observed.[137]

Another option in site-specific drug delivery is to create "immunomicelles" by attaching antibodies or antibody fragments (the Fab' fragment) to the micelles. Monoclonal antibodies can be attached, or they can be digested to obtain the Fab' fragment that can be attached by a variety of methods.[126] Polymeric micelles synthesized from polyethylene glycol–phosphatidylethanolamine (PEG-PE) conjugates have been tested and found to show higher accumulation at the tumor site than non-targeted micelles.[138]

Typically, immunomicelles such as 2C5 and 2G4 are tumor-specific, effectively binding to monolayers of antigens corresponding to their ligand.[139] It has been shown that certain monoclonal antibodies, including 2C5, are able to utilize cancer cell surface bound nucleosomes to recognize numerous tumors, but not normal cells.[140-142] Tests conducted with 2C5 labeled with Rhodamine have shown that the immunomicelle recognizes and binds to the surface of human BT20, murine LLC and El4 tumors.[139] Furthermore, the control, which consisted of micelles with no antibody, had practically no association between micelle and tumor cell. Moreover, 2C5-immunomicelles were not found to bind to any healthy cells.[140] Accumulation of 2C5-immunomicelles in murine LLC cells was found to be 30% greater than the accumulation of regular "free" micelles.[140]

In vivo tests confirmed th*e in vitro* results above and showed that micelles targeted with 2C5 monoclonal antibodies are capable of delivering the drug not only to mature tumors with a fully developed vasculature, but also to tumors in the early stages of development as well as to advanced metastatic cancers.[138] Other reports indicate that immunomicelles might be able to deliver the drug to the interior of the tumor cell via receptor-mediated endocytosis.[143]

6.3.2 Ultrasound-Triggered Release from Micelles

A scenario of an ideal drug delivery system entails the following: first, a carrier containing the drug would be injected and circulate in the blood. Then, a stimulus would be applied at a controlled location to release the drug. As mentioned, different types of stimuli have been examined, including pH, temperature, electric fields, light and ultrasound. Ultrasound has been found to be a preferred trigger mechanism due to its ability to propagate into deep tissue and to be focused directly on the target tissue.[91]

To date, there are only a few research groups working on ultrasonically controlled drug release from micelles. One is our group at Brigham Young University. Other groups include the Rapoport group at the University of Utah,[144] the Myhr group in Oslo,[145] the Phillips lab at La Trobe University in Victoria, Australia,[146] and the Mokhtari-Dizaji group in Iran.[147] The next sections review this body of literature.

6.3.2.1 Triggered Release from Micelles In Vitro

Ultrasound triggered drug release from Pluronic P105 micelles was measured under pulsed ultrasound using an ultrasonic exposure chamber with fluorescence detection illustrated in Figure 2. The study[90] examined the amount of drug release in the low frequency ultrasound range of 20

to 90 kHz. The analytical measurement in this and most studies employed the fact that many fluorescent molecules exhibit decreased fluorescence intensity when transferred from the hydrophobic core of the micelle to the aqueous environment. In this study, two intrinsically fluorescent drugs were used – Dox and Ruboxyl. The amount released was measured as a function of the applied frequency, and the most release was observed at 20 kHz. The drug release was found to decrease at higher frequencies, even when higher power densities were applied. These results indicated that the role of collapse cavitation in drug release is significant, since the MI increases as frequency decreases. That study also found that drug release increases at lower Pluronic concentrations and decreases if the drug is inserted deeper into the core of the micelle. Finally, the study also established that the drugs are re-encapsulated within the micelle between pulses of ultrasound.[90]

The kinetics of the release and re-encapsulation of Dox from Pluronic P105 micelles were studied using the same fluorescence detection exposure chamber mentioned above.[148] At a power density of 58 mW/cm^2 and a frequency of 20 kHz, experimental results showed that no significant drug release occurred from exposure to ultrasound for less than 0.1 s. This proved to be a threshold time value, above which the amount of release was proportional to the pulse length. Furthermore, it was found that re-encapsulation requires a minimum ultrasound "off" phase of 0.1 s. The maximum amount of release and re-encapsulation was observed after around 0.6 s of ultrasound. After fitting the experimental data to several models, it was found that the model of zero-order release with first-order re-encapsulation fit the experimental data best.[148] A later study showed no significant difference between the kinetic constants of acoustic release at 37 °C and 56 °C. However, the release rates of stabilized micelles proceed significantly slower when compared to non-stabilized micelles.[149]

Further investigation into the kinetics of Dox release from Pluronic P105 micelles was conducted and experimental data fitted to a more complex model that included cavitation events. The first mechanism incorporated into the model was micelle destruction, which caused the release of Dox during insonation. The micelles were destroyed because the collapsing bubble produced shock waves. The second mechanism in the model, the destruction of cavitating nuclei, showed that a small amount of Dox was re-encapsulated which initiated a slow and partial recovery phase, reassembly of micelles, and the re-encapsulation of Dox. The third mechanism was the reassembly of micelles and the fourth mechanism was the re-encapsulation of Dox. The latter two mechanisms did not show a dependence on ultrasound, but they were responsible for maintaining a steady-state drug release at a partial level and its re-encapsulation after the insonation ended. In this model, the micellar size distribution was described using a normal distribution.[150]

Experiments have also shown that ultrasound appears to disturb the interpenetrating network of the stabilized micelles, but the time constant of the degradation of the network is very long compared to the time constant related to drug release from micelles.[151] The results were used to deduce degradation kinetics of stabilized Pluronic P105 micelles. The study showed no significant difference between the network degradation time constants after one-hour exposures to 70- and 476- kHz ultrasound.[151]

Studies have also shown that the rate constant of Dox release depends on the degree of stabilization (by cross-linking). However, the re-encapsulation rate constant is roughly the same for stabilized and unstabilized micelles.[152] It has been shown that 70-kHz US releases around 2% of Dox from the core of stabilized Pluronic P105 micelles, whereas 9-10% was released from unstabilized P105 micelles.[26, 27]

Later investigations into the thermodynamic characteristics of US-activated drug release from micelles allowed the deduction of thermodynamic activation energy for micelle re-assembly and residual activation energies for micelle destruction. The model showed that residual activation energy decreased as the acoustic intensity increased. Furthermore, higher temperatures were found to increase the rate of micellar destruction but hindered the re-assembly of micelles.[152]

Artificial neural networks (ANNs) have also been used in modeling this drug delivery mechanism. As a nonlinear modeling technique, ANNs are capable of capturing and estimating the behavior exhibited by a system when exposed to various operating conditions. Some ANN control algorithms have been implemented in model predictive control (MPC).[153, 154] ANN-MPC has been shown to effectively model, control, and optimize Dox release from Pluronic P105 micelles, with feed-forward neural networks accurately capturing the dynamic behavior involved in Dox release.[97] Additionally, a controller was designed which adjusts the ultrasound frequency, intensity, and pulse length in order to ensure a constant rate of Dox release. This controller has then been successfully validated.[155]

Sensitivity analysis using the ANN model of drug release revealed that lower frequencies contribute to the most efficient Dox release, and the release increases with power density. The latter finding yet again confirms that cavitation plays an important role in US triggered drug release. Also, according to the model, drug release was not a strong function of temperature, while ANNs indicated that lower copolymer concentrations contribute to a higher rate of drug release.[156]

A solution of diblock copolymeric micelles exposed to high intensity focused ultrasound has been found to exhibit a decrease in pH. Tests conducted on samples revealed the cause of this phenomenon to be the formation of carboxylic acid dimers and hydroxyl groups. The results suggested that ultrasound induced the hydrolysis reaction of certain organic groups. Those results could be used to develop ultrasound-sensitive block copolymer micelles that have labile chemical bonds in the polymer structure. The idea is that these bonds would then be disrupted by high intensity focused ultrasound.[157]

6.3.2.2 Triggered Release to Cells In Vitro

The effect of high frequency ultrasonication on the release of Dox from Pluronic micelles and the subsequent uptake of Dox by cancer cells was studied using promyelocytic leukemia HL-60 cells, ovarian carcinoma (drug-sensitive and multi-drug resistant) cells, and breast cancer MCF-7 cells. Radical trapping was used to quantitate the cavitation events brought about by the high-frequency US. Even short exposure to high frequency ultrasound was found to greatly increase the rate of cell uptake of the antineoplastic agent.[145, 158]

The effectiveness low frequency ultrasound for triggered drug release from micelles was examined by exposing HL-60 cells to free Dox and Dox encapsulated in Pluronic P105 micelles.[159] Cells exposed to encapsulated Dox survived much longer than the cells exposed to free Dox. However, with the application of 70-kHz ultrasound, cells exposed to encapsulated Dox were killed at a faster rate than cells exposed to free Dox. These results indicated that micelles sequestered the drug from the cells, prolonging their survival, and that ultrasound released the drug from the carrier.[159]

In order to measure the uptake of Dox by HL-60 cells, 70-kHz ultrasound was pulsed in tone bursts of 0.1 sec to 2.0 sec duration.[160] The time between the bursts was also varied between 0.1 and 2.0 seconds. It was found that with constant time intervals between bursts and with a constant total insonation time, the amount of Dox uptake by the cells increased as the length of insonation increased (up to 3.0 sec). The time between bursts had no effect on the amount of uptake of the drug.[160] This indicates that Dox did not return inside the micelles, other than the amount that could have diffused back into the micelles during the period between bursts. The total calculated time to reach 90% of complete uptake was 2.5 seconds of insonation.[159]

Another in vitro study employed MDA-MB-231 breast cancer cells in addition to HL-60 cells.[146] This study also employed Dox and P105 micelles, but these micelles were stabilized by addition of disteroylphosphoethanolamine-PEG200 instead of an interpenetrating network. Encapsulation of Dox in this mixed micelle reduced Dox uptake by the MDA-MB-231 cancer cells in vitro. Application of 20-kHz ultrasound at 100 W/cm^2 released about 10% of the Dox from the micelles. However this level of insonation destroyed HL-60 cells *in vitro* at durations of more than 5 sec. However, application of 5 sec of insonation to the micelles and HL-60 cells at this power level increased the Dox uptake by the cells.

The effect of 48-kHz US on the cytotoxicity of cytosine arabinoside to HL-60 cells was examined and an increase in cell death was observed with insonation. The study ruled out hyperthermia as the cause of death as the temperature increase was less than 0.2 °C. The insonated cells were also analyzed using a scanning electron microscope, which revealed the cells to have a decreased number of microvilli and a disrupted cell surface. It was concluded that insonation disturbed and modified the cell membrane, thus increasing the amount of drug taken in by the cells.[161] Several other studies have shown similar evidence of sonoporation.[47, 162-164]

Another study showed that ultrasound formed pores on the cell surface (sonoporation) that allowed the cytoplasm of HL-60 cells to leak out of those pores.[165]

It is also important to mention here that there appears to be a synergistic effect between chemotherapy drugs and ultrasound. A study has shown that exposure to ultrasound that lasted one hour rendered Dox significantly more toxic to Chinese hamster lung cancer.[160] Next we examine literature reporting *in vivo* drug release.

6.3.2.3 Triggered Release in Animal Models

There is a synergistic effect between chemotherapy drugs and ultrasound even in the absence of micelles. Several studies have shown that tumor growth was slowed by exposure to ultrasound and free drug[166] or liposomal drug.[24, 145, 167, 168]

For example, our research group used a tumor-bearing rat model to investigate the effect of ultrasound and micellar drugs on tumor growth rate and to determine which frequency works best in the treatment. It was found that the combination of drug and ultrasound resulted in a slower tumor growth rate than free drug without US. It was also found that ultrasound frequency does not affect the growth rate, as 20- and 478-kHz treatments yielded the same results.[159]

Another *in vivo* study was conducted using 42 rats, which were inoculated in each hind leg with a colon carcinogen DHD/K12/TRb tumor cell line. Six weeks after tumor inoculation, Dox encapsulated in stabilized Pluronic P105 micelles, was administered weekly by intravenous infusion.[168] Ultrasound was applied about 30 minutes after infusion, allowing time for the micelles to begin accumulating at the tumor site. The study showed that Dox concentrations of 8 mg/kg were lethal within two weeks, while 5.33 and 4.0 mg/kg were lethal within six weeks. Concentrations of 1.33 and 2.67 mg/kg did not cause death. The general results looked

promising, as the tumors that were exposed to a combination of encapsulated Dox and US grew slower than the tumors not exposed to ultrasound; some US-treated tumors actually regressed. In treated rats the distribution of Dox to various organs and tissues was measured, and more Dox was found in US-treated tumors than the contralateral untreated tumors. Furthermore, the drug was retained in the tumors longer and in higher concentrations than in other tissues, which suggests drug accumulation by the EPR effect with a maximum in concentration at about 12 hrs.[169]

Similar studies have been done in mouse models. Tumors exposed to ultrasound and Dox-containing micelles accumulated a significantly greater amount of micelles than non-insonated tumors.[170] The same study reported that the cardiotoxicity of Dox is reduced by the use of micelles as the encapsulated Dox did not accumulate as much in the heart of the mice. Delivery and effectiveness of 5-fluorouracil (5FU) was also studied in a mouse model of colon cancer.[145] Tumor reduction was significant when the micellar delivery was combined with 20-kHz ultrasound at 3.16 W/cm^2 for 30 minutes.

In another mouse model, this time of breast cancer, ultrasonic frequencies of 28 kHz and 3 MHz were applied simultaneously to a tumor after intravenous administration of Dox in stabilized P105 micelles.[147] The biodistribution of Dox was compared to that when the micelles were not insonated and when free Dox was employed. The Dox concentrations in various tissues were measured 24 hrs after treatment. The mice receiving micellar Dox with ultrasound had nearly nine times more Dox in their tumors than mice receiving free Dox, and more than three times the amount of mice receiving micellar Dox without insonation. The Dox concentration in other tissues was less with micellar Dox than free Dox. This study supports the hypothesis that micellar Dox is extravasated in the tumor, and that insonation of the tumor further increases Dox

retention and/or uptake in the tumor tissue. Other studies showed that US alone appears to increase extravasation.[30, 171, 172]

6.3.2.4 Mechanisms of Ultrasonic-Activated Delivery from Micelles

It is important to examine the mechanism by which micelles deliver anti-cancer drugs with and without ultrasound. First, micelles slowly and continually release drug. Thus if they collect in a tumor tissue via the EPR effect, release will occur to the exterior of the cells. The drug may then diffuse into the cells or enter by other pathways. A second mechanism is that micelles may be taken into the cell by endocytosis, a process by which a cell internalizes macromolecules and fluid from its surroundings. Two types of endocytosis exist: pinocytosis and receptor-mediated endocytosis. Pinocytosis is characterized by the uptake of small droplets of extracellular fluid, and any material dissolved in it. Receptor-mediated endocytosis, as the name suggests, utilizes a specific receptor on the cell membrane surface. This receptor binds to the target molecule, or ligand, which in turn sends a signal to the cell membrane to fold in on itself, forming a small vesicle through which the molecule is internalized. Micelles can be labeled with a targeting ligand, such as folate or anti-HER2 mAb, that induces endocytosis of the ligand and its attached micelle.[136]

When ultrasound is applied, additional uptake mechanisms come into play. Firstly, US can enhance the release rate of drug from micelles, which will be discussed thoroughly below. When US induces drug release from micelles, there is a higher concentration of external drug that can diffuse into the cell or enter by pinocytosis. If cavitation events sonoporate the cell membrane, released drug can diffuse directly into the cell, or whole micelles could diffuse in.[96] On a global scale, US appears to enhance extravasation, bringing more micelles into the tumor interstitium.[30, 171, 172]

Investigation into the mechanisms of ultrasonic drug delivery to cancer cells was conducted in an attempt to elucidate which of these mechanisms was mainly implicated in ultrasonic drug delivery from micelles. First, let's consider the shielding or protection effect that Pluronic P105 micelles have on the drug's cytotoxicity. Below the critical micellar concentration (CMC), one study showed that the uptake of fluorescently-labeled Pluronic micelles by HL-60 cells was proportional to the concentration present in the incubation medium.[96] Above the CMC, intracellular uptake of the micelles was far less efficient. These findings led to conclude that Pluronic micelles are internalized through fluid-phase endocytosis, rather than by diffusion through plasma membranes. The experiments were conducted using flow cytometry, fluorescence spectroscopy, and confocal and fluorescence microscopy.

While US apparently upregulates endocytosis in endothelial cells[173] and fibroblasts,[174] the increased accumulation of Dox in HL-60 cells was not due to increased endocytosis stimulated by ultrasonication.[175] Rather, it was suspected that sonoporation played the most important role in the process. This led to several hypotheses being proposed as to how ultrasound increases the rate of uptake of the drug by the cells.

One hypothesis states that acoustic streaming, or momentum transfer from sound waves to the biological fluid, and microconvection created by oscillating bubbles of gas in the liquid are responsible for the disruption of the cell membrane. The perturbed cell membrane is rendered more permeable to the drug. We have discussed this concept in section 2.1.3; briefly, if the bubbles do not exhibit complete collapse during their shrinkage cycle, then stable cavitation creates high velocity gradients. But collapse cavitation also creates high shear stresses, which can sonoporate the cell membrane.[175] The micelles also experience the same high shear stresses. There is a strong correlation between the amount of drug release and subharmonic acoustic

emissions, which is attributed to collapse cavitation that disturbs the micelle structure and results in the release of the drug (see Figure 1).[27] On a related note, our group has shown that increasing the static pressure suppresses bubble cavitation and drug release,[176] again supporting the hypothesis that bubble cavitation causes drug release. Thus acoustic streaming and microconvection play very minor roles, if any at all.

Another hypothesis states that exposure to ultrasound increases the concentration of the drug (due to its release from micelles), but does not alter the permeability of the cell membrane. The high concentration outside the cell membrane creates a sufficiently high diffusion gradient for drug uptake by the cells. However, this hypothesis was dismissed when several studies demonstrated that ultrasound does indeed increase the permeability of the cell membrane.[175]

Micelles are transported into cancer cells via endocytosis, and the third hypothesis states that ultrasound increases the rate of endocytosis. Experiments have revealed that while ultrasound enhances drug uptake by cells, the rate of endocytosis is not enhanced, so this hypothesis was also dismissed.[175] Experiments support the possibility of this hypothesis, in that US does appear to enhance endocytosis in some cell lines, [173, 174] but not all cell lines.[175] Direct experimental uptake of micelles by US-enhanced endocytosis has not yet been observed.

The conclusion of this subsection is that acoustically activated micellar drug delivery systems are rendered effective due to two main mechanisms. Ultrasound causes drug release from the micelles as it disrupts the core of polymeric micelles, most probably by strong shear stresses; and additionally, ultrasonic sonoporation has been shown to form micropores in the membranes of cancer cells, which allows released drugs or whole micelles to passively diffuse into the cells.[84] Enhanced endocytosis is a possibility.

Additional studies showed drug uptake could be characterized by Langmuir-type isotherms, which implies that the system has a restricted number of sorption units.[158] Thus, the phenomenon of increased free drug uptake upon sonication could be attributed to new sorption centers being formed as cell structures are perturbed. It could also be that as the equilibrium between the drug inside the cells and the drug outside is shifted, excited drug molecules are generated. This excitation would increase the enthalpy of the drug internalization process.[158]

Once the micelle and drug molecules are taken up with the cell, the objective is for Dox to accumulate in the nucleus, intercalate into the DNA bases, and affect many of the cell functions– primarily DNA replication. As a topoisomerase inhibitor, Dox is capable of causing single and double strand breaks in the DNA of treated cells. Therefore, the next paragraph will summarize the results of using the comet assay to measure the amount of DNA damage.

The comet assay was used to quantify DNA damage by measuring the length and the fraction of broken DNA strands. The pattern of DNA damage indicates the mode of cell death.[177] Experiments were conducted in which cells were treated with various combinations of Dox, US, and Pluronic P105 micelles. The cells were sonicated and lysed, then placed in an electrophoresis buffer, which resulted in DNA unwinding, after which electrophoresis was performed. Electrophoresis displayed the migration of intrinsically negative DNA away from the negative electrode and towards the positive electrode. Then a distilled water bath was used to re-anneal the DNA, which was then stained with propidium iodide, a fluorescent dye. Upon analysis, the electrophoresed DNA looks like a comet, with the damaged DNA migrating forming the tail, and undamaged DNA forming the head.[178] The results showed that ultrasound alone was found to cause negligible damage to DNA, whether with or without P105. Dox contained in P105 caused no damage unless US was applied, and free Dox and Dox with ultrasound display various

degrees of damage. The rate of DNA damage was higher when a combination of Dox, P105, and US were applied, and a slower rate was observed when Dox and US were used, and there was an even slower rate with free Dox.[175] Another study showed that apoptosis was the mode of cell death in ultrasonic Dox delivery from P105 micelles.[178] The conclusion was reached after examining DNA fragmentation pattern of cells exposure to US and encapsulated Dox.

In conclusion, polymeric micelles are proven drug carriers that can be activated by ultrasound to release their payload of drugs. By sequestering and then releasing with the ultrasonic trigger, drug delivery can be controlled in time and space so the adverse side effects of chemotherapy can be minimized. Pluronic P105 micelles have been successful in encapsulating and then acoustically releasing at least 3 chemotherapy agents. These micelles and their stabilized derivatives have also shown promise as viable delivery vehicles in vitro and in vivo. The question to be answered next is whether these micelles are efficient at higher ultrasonic frequencies that are easy to focus but are less capable of penetrating deep tissues.

6.4 The Future of Ultrasound-Triggered Drug Delivery from Micelles

Definitely the future of ultrasonically activated drug delivery from nanovehicles is bright. Ultrasound presents unprecedented non-invasive control of a fairly effective trigger. In the race to the clinic, ultrasound-triggered release from micelles is in competition with release from liposomes, polymersomes and other nanovehicles. When comparing triggered release from micelles and from liposomes, micelles have advantages in ease of manufacturing (self-assembly) and small size, but they have disadvantages in non-perfect sequestration (drug can slowly leak

out) and incomplete release. Researchers and pharmaceutical companies must evaluate and select the best methods also in terms of manufacturing cost, quality control, product stability, shelf life, consumer safety, and more. As mentioned, the great advantage of these micellar systems is that they are self-assembled, so they are inherently stable and do not disassemble upon prolonged storage. In theory they can be lyophilized and reconstituted by the addition of water or saline, since they self-assemble. There remains much research to perform regarding manufacturing, storage and administration.

It follows, therefore, that for micellar systems to compete with liposomal systems, one needs to develop more effective sequestration in combination with more sensitivity to shear-stress induced release. This is a difficult conundrum to solve. Designing the core to attract the therapeutic more securely would decrease premature leakage, but would make the core less susceptible to rupture by shear stress, keep the therapeutic associated with the hydrophobic sites on the micellar molecules, and increase the rate of re-encapsulation once the micelle recovers from the shear assault. Some creative molecular design will be involved.

Another approach would be to create more cavitation events near the micelles to increase the shear stress on the micelle. For example, one could increase the amount of ultrasonic cavitation by providing extrinsic bubbles, such as perfluoropropane microbubbles that are fairly stable in blood and that are used as ultrasound contrast agents. Even better, the micelles could be attached directly to the surface of the microbubbles using the same conjugation chemistry employed to attach liposomes to microbubbles.[179, 180] The size of the gas bubbles restricts delivery to the lumen of the vascular system, but these assemblies could be targeted to collect on diseased tissues of the circulatory system. Then the application of ultrasound could collapse the bubble supporting the micelles, creating high shear stress on the micelles and on the adjacent diseased

tissue cells. This scenario would produce more concentrated release since all micelles are guaranteed to be in the immediate vicinity of a collapsing bubble.

This delivery technique could be modified for delivery beyond the vascular system by attaching the micelles to nanoemulsions of perfluorocarbon liquids, such as perfluoropentane, stabilized by polymer or other surfactants.[51, 52, 114, 181, 182] These assemblies could be built sufficiently small to pass through the fenestrations in the malformed vasculature of tumors and collect in tumor tissues. Once on site, the application of ultrasound could transform the superheated perfluoropentane into a gas bubble in the tissue, which would upon further insonation collapse and rupture the attached micelles.

Needless to say, there are many opportunities for creative science in ultrasound-triggered delivery from micelles. And while the scientific community has not reached a perfect or ideal acoustically activated micellar drug delivery system, we believe that we are moving forward towards this goal.

References

1. C. S. S. R. Kumar and F. Mohammad, *Advanced Drug Delivery Reviews*, 2011, **63**, 789-808.
2. S. Power, M. M. Slattery and M. J. Lee, *Cardiovasc Inter Rad*, 2011, **34**, 676-690.
3. A. P. Esser-Kahn, S. A. Odom, N. R. Sottos, S. R. White and J. S. Moore, *Macromolecules*, 2011, **44**, 5539-5553.
4. L. H. Lindner and M. Hossann, *Curr Opin Drug Disc*, 2010, **13**, 111-123.
5. Y. Bae and K. Kataoka, *Advanced Drug Delivery Reviews*, 2009, **61**, 768-784.
6. A. Chilkoti, M. R. Dreher, D. E. Meyer and D. Raucher, *Advanced Drug Delivery Reviews*, 2002, **54**, 613-630.

7. K. J. Yoon, P. M. Potter and M. K. Danks, *Curr Med Chem Anticancer Agents*, 2005, **5**, 107-113.
8. K. Ashihara, K. Kurakata, T. Mizunami and K. Matsushita, *Acoustical Science and Technology*, 2006, **27**, 12-19.
9. D. A. Christensen, *Ultrasonic Bioinstrumentation*, Wiley, New York, 1988.
10. S. A. Goss, R. L. Johnston and F. Dunn, *J. Acoust. Soc. Am.*, 1980, **68**, 93-108.
11. S. A. Goss, R. L. Johnston and F. Dunn, *J. Acoust. Soc. Am.*, 1978, **64**, 423-453.
12. T. G. Leighton, *Prog Biophys Mol Bio*, 2007, **93**, 3-83.
13. C. E. Brennen, *Cavitation and Bubble Dynamics*, Oxford University Press, New York, 1995.
14. J. Wu, *Prog. Biophys. Molec. Biol.*, 2007, **93**, 363-373.
15. J. R. Wu and W. L. Nyborg, *Advanced Drug Delivery Reviews*, 2008, **60**, 1103-1116.
16. E. S. Richardson, W. G. Pitt and D. J. Woodbury, *Biophysical Journal*, 2007, **93**, 4100-4107.
17. T. G. Leighton, *The Acoustic Bubble*, Academic Press, London, 1994.
18. E. B. Flint and K. S. Suslick, *Science*, 1991, **253**, 1397-1399.
19. W. B. McNamara, Y. T. Didenko and K. S. Suslick, *Nature*, 1999, **401**, 772-775.
20. L. Somaglino, G. Bouchoux, J. L. Mestas and C. Lafon, *Ultrason Sonochem*, 2011, **18**, 810-810.
21. T. J. Mason, J. P. Lorimer, D. M. Bates and Y. Zhao, *Ultrason Sonochem*, 1994, **1**, S91-S95.
22. L. Villeneuve, L. Alberti, J. P. Steghens, J. M. Lancelin and J. L. Mestas, *Ultrason Sonochem*, 2009, **16**, 339-344.
23. G. J. Price, F. A. Duck, M. Digby, W. Holland and T. Berryman, *Ultrason Sonochem*, 1997, **4**, 165-171.
24. A. Schroeder, J. Kost and Y. Barenholz, *Chemistry and Physics of Lipids*, 2009, **162**, 1-16.
25. A. Schroeder, Y. Avnir, S. Weisman, Y. Najajreh, A. Gabizon, Y. Talmon, J. Kost and Y. Barenholz, *Langmuir*, 2007, **23**, 4019-4025.
26. G. A. Husseini, M. A. Diaz de la Rosa, T. Gabuji, Y. Zeng, D. A. Christensen and W. G. Pitt, *J. Nanosci. Nanotech.*, 2007, **7**, 1-6.
27. G. A. Husseini, M. A. Diaz, E. S. Richardson, D. A. Christensen and W. G. Pitt, *J. Controlled Release*, 2005, **107**, 253-261.
28. D. M. Hallow, A. D. Mahajan and M. R. Prausnitz, *J. Controlled Release*, 2007, **118**, 285-293.
29. C. Y. Lin, Y. L. Huang, J. R. Li, F. H. Chang and W. L. Lin, *Ultrasound in Medicine and Biology*, 2010, **36**, 1460-1469.
30. S. M. Stieger, C. F. Caskey, R. H. Adamson, S. P. Qin, F. R. E. Curry, E. R. Wisner and K. W. Ferrara, *Radiology*, 2007, **243**, 112-121.
31. M. A. O'Reilly, A. C. Waspe, M. Ganguly and K. Hynynen, *Ultrasound in medicine & biology*, 2011, **37**, 587-594.
32. E. E. Cho, J. Drazic, M. Ganguly, B. Stefanovic and K. Hynynen, *J Cereb Blood Flow Metab*, 2011, **31**, 1852-1862.
33. K. Hynynen, *Methods Mol Biol*, 2009, **480**, 175-185.
34. K. Hynynen, *Advanced Drug Delivery Reviews*, 2008, **60**, 1209-1217.
35. S. Meairs and A. Alonso, *Prog Biophys Mol Bio*, 2007, **93**, 354-362.
36. C. S. Yoon and J. H. Park, *Expert Opin Drug Del*, 2010, **7**, 321-330.
37. L. Zhang and Z. B. Wang, *Front Med China*, 2010, **4**, 294-302.
38. M. Fatar, M. Stroick, M. Griebe, A. Alonso, S. Kreisel, R. Kern, M. G. Hennerici and S. Meairs, *Ultrasound in Medicine and Biology*, 2008, **34**, 1414-1420.
39. A. F. Prokop, A. Soltani and R. A. Roy, *Ultrasound in Medicine and Biology*, 2007, **33**, 924-933.
40. A. V. Alexandrov, C. A. Molina, J. C. Grotta, Z. Garami, S. R. Ford, J. Alvarez-Sabin, J. Montaner, M. Saqqur, A. M. Demchuk, L. A. Moye, M. D. Hill, A. W. Wojner, F. Al-Senani, S. Burgin, S. Calleja, M. Campbell, C. I. Chen, O. Chernyshev, J. Choi, A. El-Mitwalli, R. Felberg, S. Ford, Z. Garami, W. Irr, J. Grotta, C. Hall, Y. Iguchi, J. Ireland, L. Labiche, M. Malkoff, L. Morgenstern, E.

Noser, N. Okon, P. Piriyawat, D. Robinson, H. Shaltoni, S. Shaw, K. Uchino, F. Yatsu, J. Alvarez-Sabin, J. F. Arenillas, R. Huertas, C. Molina, J. Montaner, M. Ribo, M. Rubiera, E. Santamarina, M. Saqqur, N. Alchtar, F. O'Rourke, S. Hussain, A. Shuaib, E. Abdalla, A. Demchuk, K. Fischer, M. D. Hill, J. Kennedy, J. Roy, K. J. Ryckborst, M. Schebel and C. Investigators, *New Engl J Med*, 2004, **351**, 2170-2178.

41. C. W. Francis, *Echocardiogr-J Card*, 2001, **18**, 239-246.
42. E. Biagi, L. Breschi, E. Vannacci and L. Masotti, *Ieee Transactions on Ultrasonics Ferroelectrics and Frequency Control*, 2007, **54**, 480-497.
43. E. Sassaroli and K. Hynynen, *Ultrasound in Medicine and Biology*, 2007, **33**, 1651-1660.
44. R. E. Apfel and C. K. Holland, *Ultrasound Med. Biol.*, 1991, **17**, 179-185.
45. S. B. Barnett, G. R. Ter Haar, M. C. Ziskin, H. D. Rott, F. A. Duck and K. Maeda, *Ultrasound in Medicine and Biology*, 2000, **26**, 355-366.
46. W. L. Nyborg, *Ultrasound Med. Biol.*, 2001, **27**, 301-333.
47. P. Prentice, A. Cuschierp, K. Dholakia, M. Prausnitz and P. Campbell, *Nat Phys*, 2005, **1**, 107-110.
48. P. Marmottant and S. Hilgenfeldt, *Nature*, 2003, **423**, 153-156.
49. Y. Wang, X. Li, Y. Zhou, P. Huang and Y. Xu, *Int J Pharm*, 2010, **384**, 148-153.
50. J. R. Lattin, D. M. Belnap and W. G. Pitt, *Colloids and Surfaces B: Biointerfaces*, 2012, **89**, 93-100.
51. P. S. Sheeran, S. Luois, P. A. Dayton and T. O. Matsunaga, *Langmuir : the ACS journal of surfaces and colloids*, 2011, **27**, 10412-10420.
52. P. S. Sheeran, V. P. Wong, S. Luois, R. J. McFarland, W. D. Ross, S. Feingold, T. O. Matsunaga and P. A. Dayton, *Ultrasound in medicine & biology*, 2011, **37**, 1518-1530.
53. N. Y. Rapoport, A. L. Efros, D. A. Christensen, A. M. Kennedy and K.-H. Nam, *Bubble Science Eng Tech*, 2009, **1**, 31-39.
54. R. N. Singh, G. A. Husseini and W. G. Pitt, *Ultrason Sonochem*, 2012, **in press**.
55. H. C. Starritt, F. A. Duck and V. F. Humphrey, *Ultrasound Med Biol*, 1989, **15**, 363-373.
56. M. J. Shortencarier, P. A. Dayton, S. H. Bloch, P. A. Schumann, T. O. Matsunaga and K. W. Ferrara, *Ieee Transactions on Ultrasonics Ferroelectrics and Frequency Control*, 2004, **51**, 822-831.
57. M. C. Ziskin and S. B. Barnett, *ultrasound in Med. & Biol.*, 2001, **27**, 875-876.
58. S. B. Barnett, H.-D. Rott, G. R. t. Haar, M. C. Ziskin and K. Maeda, *Ultrasound Med. Biol.*, 1997, **23**, 805-812.
59. S. B. Barnett, G. R. T. Haar, M. C. Ziskin, H.-D. Rott, F. A. Duck and K. Maeda, *Ultrasound in Med. & Biol.*, 2000, **26**, 355-366.
60. D. Miller, P. Li and W. F. Armstrong, *Echocardiogr-J Card*, 2004, **21**, 125-132.
61. A. M. Rediske, B. L. Roeder, M. K. Brown, J. L. Nelson, R. L. Robison, D. O. Draper, G. B. Schaalje, R. A. Robison and W. G. Pitt, *Antimicrob. Agents Chemother.*, 1999, **43**, 1211-1214.
62. T. Nishioka, H. Luo, M. C. Fishbein, B. Cercek, J. S. Forrester, C. J. Kim, H. Berglund and R. J. Siegel, *J Am Coll Cardiol*, 1997, **30**, 561-568.
63. A. M. Rediske, B. L. Roeder, J. L. Nelson, R. L. Robison, G. B. Schaalje, R. A. Robison and W. G. Pitt, *Antimicrob. Agents Chemother.*, 2000, **44**, 771-772.
64. H. Luo, Y. Birnbaum, M. C. Fishbein, T. M. Peterson, T. Nagai, T. Nishioka and R. J. Siegel, *Thromb Res*, 1998, **89**, 171-177.
65. L. Sicard-Rosenbaum, D. Lord, J. V. Danoff, A. K. Thom and M. A. Eckhaus, *Physical Ther.*, 1995, **75**, 3-13.
66. L. Sicard-Rosenbaum, J. V. Danoff, J. A. MGuthrie and M. A. Eckhaus, *Physical Therapy*, 1998, **78**, 217-277.
67. D. L. Miller and C. Y. Dou, *J Ultras Med*, 2005, **24**, 349-354.

68. C. Oerlemans, W. Bult, M. Bos, G. Storm, J. F. W. Nijsen and W. E. Hennink, *Pharmaceutical Research*, 2010, **27**, 2569-2589.
69. M. C. Jones and J. C. Leroux, *Eur J Pharm Biopharm*, 1999, **48**, 101-111.
70. S. Stolnic, L. Illum and S. S. Davis, *Advanced Drug delivery Reviews*, 1995, **16**, 195-214.
71. S. I. Jeon, J. H. Lee, J. D. Andrade and P. G. DeGennes, *J. Colloid Interface Sci.*, 1991, **142**, 149-158.
72. J. C. Leroux, P. Gravel, L. Balant, B. Volet, B. M. Anner, E. Allemann, E. Doelker and R. Gurny, *J Biomed Mater Res*, 1994, **28**, 471-481.
73. A. Misra, K. Florence, M. Lalan and T. Shah, in *Colloids in Drug Delivery*, ed. M. Fanun, CRC Press, Boca Raton, FL, 2010.
74. V. P. Torchilin, *Pharmaceutical Research*, 2007, **24**, 1-16.
75. G. S. Kwon and K. Kataoka, *Advanced Drug Delivery Reviews*, 1995, **16**, 295-309.
76. M. Yokoyama, T. Sugiyama, T. Okano, Y. Sakurai, M. Naito and K. Kataoka, *Pharmac. Res.*, 1993, **10**, 895-899.
77. M. Yokoyama, T. Okano, Y. Sakurai, H. Ekimoto, C. Shibazaki and K. Kataoka, *Cancer Res.*, 1991, **51**, 3229-3236.
78. G. S. Kwon, M. Yokoyama, T. Okano, Y. Sakurai and K. Kataoka, *Pharmac. Res.*, 1993, **10**, 970-974.
79. E. V. Batrakova, S. Li, A. M. Brynskikh, A. K. Sharma, Y. L. Li, M. Boska, N. Gong, R. L. Mosley, V. Y. Alakhov, H. E. Gendelman and A. V. Kabanov, *Journal of Controlled Release*, 2010, **143**, 290-301.
80. D. Y. Alakhova, N. Y. Rapoport, E. V. Batrakova, A. A. Timoshin, S. Li, D. Nicholls, V. Y. Alakhov and A. V. Kabanov, *Journal of Controlled Release*, 2010, **142**, 89-100.
81. E. V. Batrakova and A. V. Kabanov, *Journal of Controlled Release*, 2008, **130**, 98-106.
82. A. Rolland, J. O'Mullane, P. Goddard, L. Brookman and K. Petrak, *J. Appl. Polym. Sci.*, 1992, **44**, 1195-1203.
83. P. Alexandridis, J. F. Holzwarth and T. A. Hatton, *Macromolecules*, 1994, **27**, 2414-2425.
84. G. A. Husseini and W. G. Pitt, *J Pharm Sci*, 2009, **98**, 795-811.
85. N. Rapoport and K. Caldwell, *Colloids and Surfaces B: Biointerfaces*, 1994, **3**, 217-228.
86. N. Munshi, N. Rapoport and W. G. Pitt, *Cancer Letters*, 1997, **117**, 1-7.
87. J. D. Pruitt, G. Husseini, N. Rapoport and W. G. Pitt, *Macromolecules*, 2000, **33**, 9306-9309.
88. G. A. Husseini, R. I. El-Fayoumi, K. L. O'Neill, N. Y. Rapoport and W. G. Pitt, *Cancer Letters*, 2000, **154**, 211-216.
89. G. A. Husseini, D. A. Christensen, N. Y. Rapoport and W. G. Pitt, *J. Controlled Rel.*, 2002, **83**, 302-304.
90. G. A. Husseini, G. D. Myrup, W. G. Pitt, D. A. Christensen and N. Y. Rapoport, *J. Controlled Release*, 2000, **69**, 43-52.
91. H. Zhang, H. Xia, J. Wang and Y. Li, *Journal of controlled release : official journal of the Controlled Release Society*, 2009, **139**, 31-39.
92. N. Rapoport, A. I. Smirnov, A. Timoshin, A. M. Pratt and W. G. Pitt, *Archives Biochem. Biophys.*, 1997, **344**, 114-124.
93. N. Rapoport, *Colloids Surfaces B: Biointerfaces*, 1999, **16**, 93-111.
94. N. Rapoport and L. Pitina, *J. Pharm. Sci.*, 1998, **87**, 321-325.
95. N. Y. Rapoport, J. N. Herron, W. G. Pitt and L. Pitina, *J Controlled Rel*, 1999, **58**, 153-162.
96. M. D. Muniruzzaman, A. Marin, Y. Luo, G. D. Prestwich, W. G. Pitt, G. Husseini and N. Y. Rapoport, *Colloids and Surfaces B: Biointerfaces*, 2002, **25**, 233-241.
97. G. A. Husseini, N. M. Abdel-Jabbar, F. S. Mjalli, W. G. Pitt and A. Al-Mousa, *J Franklin I*, 2011, **348**, 1276-1284.
98. J. R. Eisenbrey, O. M. Burstein, R. Kambhampati, F. Forsberg, J. B. Liu and M. A. Wheatley, *Journal of controlled release : official journal of the Controlled Release Society*, 2010, **143**, 38-44.

99. Z. Y. Hu, F. Luo, Y. F. Pan, C. Hou, L. F. Ren, J. J. Chen, J. W. Wang and Y. D. Zhang, *J Biomed Mater Res A*, 2008, **85A**, 797-807.
100. C. Y. Zhan, B. Gu, C. Xie, J. Li, Y. Liu and W. Y. Lu, *Journal of Controlled Release*, 2010, **143**, 136-142.
101. Y. Zeng and W. G. Pitt, *J. Biomater. Sci. Polymer Edn.*, 2006, **17**, 591-604.
102. M. Gou, X. Zheng, K. Men, J. Zhang, B. Wang, L. Lv, X. Wang, Y. Zhao, F. Luo, L. Chen, X. Zhao, Y. Wei and Z. Qian, *Pharmaceutical Research*, 2009, **26**, 2164-2173.
103. A. S. Mikhail and C. Allen, *Biomacromolecules*, 2010, **11**, 1273-1280.
104. M. L. Forrest, J. A. Yanez, C. M. Remsberg, Y. Ohgami, G. S. Kwon and N. M. Davies, *Pharmaceutical Research*, 2008, **25**, 194-206.
105. L. Zheng, M. Gou, S. Zhou, T. Yi, Q. Zhong, Z. Li, X. He, X. Chen, L. Zhou, Y. Wei, Z. Qian and X. Zhao, *Oncology Reports*, 2011, **25**, 1557-1564.
106. K. Kataoka, A. Harada and Y. Nagasaki, *Advanced Drug Delivery Reviews*, 2001, **47**, 113-131.
107. C. Li and S. Wallace, *Advanced Drug Delivery Reviews*, 2008, **60**, 886-898.
108. T. Minko, P. Kopeckova and J. Kopecek, *Int J Cancer*, 2000, **86**, 108-117.
109. M. Campone, J. M. Rademaker-Lakhai, J. Bennouna, S. B. Howell, D. P. Nowotnik, J. H. Beijnen and J. H. M. Schellens, *Cancer Chemotherapy and Pharmacology*, 2007, **60**, 523-533.
110. T. Nakanishi, S. Fukushima, K. Okamoto, M. Suzuki, Y. Matsumura, M. Yokoyama, T. Okano, Y. Sakurai and K. Kataoka, *Journal of Controlled Release*, 2001, **74**, 295-302.
111. C. Li, J. E. Price, L. Milas, N. R. Hunter, S. Ke, D. F. Yu, C. Charnsangavej and S. Wallace, *Clin Cancer Res*, 1999, **5**, 891-897.
112. E. Auzenne, N. J. Donato, C. Li, E. Leroux, R. E. Price, D. Farquhar and J. Klostergaard, *Clin Cancer Res*, 2002, **8**, 573-581.
113. J. W. Singer, S. Shaffer, B. Baker, A. Bernareggi, S. Stromatt, D. Nienstedt and M. Besman, *Anti-Cancer Drug*, 2005, **16**, 243-254.
114. N. Rapoport, K. H. Nam, R. Gupta, Z. G. Gao, P. Mohan, A. Payne, N. Todd, X. Liu, T. Kim, J. Shea, C. Scaife, D. L. Parker, E. K. Jeong and A. M. Kennedy, *Journal of Controlled Release*, 2011, **153**, 4-15.
115. Y. H. Bae and K. Park, *Journal of controlled release : official journal of the Controlled Release Society*, 2011, **153**, 198-205.
116. H. C. Shin, A. W. G. Alani, D. A. Rao, N. C. Rockich and G. S. Kwon, *Journal of Controlled Release*, 2009, **140**, 294-300.
117. S. R. Croy and G. S. Kwon, *Curr Pharm Design*, 2006, **12**, 4669-4684.
118. Y. Bae, T. A. Diezi, A. Zhao and G. S. Kwon, *Journal of Controlled Release*, 2007, **122**, 324-330.
119. Z. G. Gao, H. D. Fain and N. Rapoport, *Journal of Controlled Release*, 2005, **102**, 203-222.
120. G. Gaucher, M. H. Dufresne, V. P. Sant, N. Kang, D. Maysinger and J. C. Leroux, *Journal of Controlled Release*, 2005, **109**, 169-188.
121. N. Rapoport, *Prog Polym Sci*, 2007, **32**, 962-990.
122. G. Kwon, M. Naito, M. Yokoyama, Y. Sakurai, T. Okano and K. Kataoka, *Langmuir*, 1993, **9**, 945-949.
123. K. Kataoka, T. Matsumoto, M. Yokoyama, T. Okano, Y. Sakurai, S. Fukushima, K. Okamoto and G. S. Kwon, *J. Controlled Release*, 2000, **64**, 143-153.
124. G. S. Kwon, M. Yokoyama, T. Okano, Y. Sakurai and K. Kataoka, *Journal of Controlled Release*, 1994, **28**, 334-335.
125. B. Stella, S. Arpicco, M. T. Peracchia, D. Desmaele, J. Hoebeke, M. Renoir, J. D'Angelo, L. Cattel and P. Couvreur, *J Pharm Sci*, 2000, **89**, 1452-1464.
126. L. Nobs, F. Buchegger, R. Gurny and E. Allemann, *J Pharm Sci*, 2004, **93**, 1980-1992.
127. S. Hirota and N. Duzgunes, *Curr Drug Discov Technol*, 2011, **8**, 286.
128. P. Ghosh, B. K. Bachhawat and A. Surolia, *Arch Biochem Biophys*, 1981, **206**, 454-457.

129. R. J. Lee and P. S. Low, *Bba-Biomembranes*, 1995, **1233**, 134-144.
130. J. Yang, C.-H. Lee, J. Park, S. Seo, E.-K. Lim, Yong Jin Song, J.-S. Suh, H.-G. Yoon, Y.-M. Huh and S. Haam, *J. Mater. Chem.*, 2007, **17**, 2695-2699.
131. A. Hayama, T. Yamamoto, M. Yokoyama, K. Kawano, Y. Hattori and Y. Maitani, *J Nanosci Nanotechnol*, 2007, **8**, 1-6.
132. Y. Bae, N. Nishiyama and K. Kataoka, *Bioconjugate Chem*, 2007, **18**, 1131-1139.
133. E. S. Lee, K. Na and Y. H. Bae, *J. Controlled Release*, 2003, **91**, 103-113.
134. H. S. Yoo and T. G. Park, *Journal of Controlled Release*, 2004, **96**, 273-283.
135. E. K. Park, S. Y. Kim, S. B. Lee and Y. M. Lee, *Journal of Controlled Release*, 2005, **109**, 158-168.
136. S. J. Huang, S. L. Sun, T. H. Feng, K. H. Sung, W. L. Lui and L. F. Wang, *Eur J Pharm Sci*, 2009, **38**, 64-73.
137. N. V. Nukolova, H. S. Oberoi, S. M. Cohen, A. V. Kabanov and T. K. Bronich, *Biomaterials*, 2011, **32**, 5417-5426.
138. A. N. Lukyanov, Z. Gao and V. P. Torchilin, *Journal of Controlled Release* 2003, **91**, 97-102.
139. V. P. Torchilin, A. N. Lukyanov, Z. Gao and B. Papahadjopoulos-Sternberg, *P Natl Acad Sci USA*, 2003, **100**, 6039-6044.
140. L. Z. Iakoubov and V. P. Torchilin, *Oncol Res*, 1997, **9**, 439-446.
141. L. Iakoubov, O. Rokhlin and V. Torchilin, *Immunol Lett*, 1995, **47**, 147-149.
142. L. Z. Iakoubov and V. P. Torchilin, *Cancer Detect Prev*, 1998, **22**, 470-475.
143. J. W. Park, D. B. Kirpotin, K. Hong, R. Shalaby, Y. Shao, U. B. Nielsen, J. D. Marks, D. Papahadjopoulos and C. C. Benz, *Journal of Controlled Release*, 2001, **74**, 95-113.
144. P. Mohan and N. Rapoport, *Mol Pharmaceut*, 2010, **7**, 1959-1973.
145. G. Myhr and J. Moan, *Cancer Letters*, 2006, **232**, 206-213.
146. M. Ugarenko, C. K. Chan, A. Nudelman, A. Rephaeli, S. M. Cutts and D. R. Phillips, *Oncol Res*, 2009, **17**, 283-299.
147. H. Hasanzadeh, M. Mokhtari-Dizaji, S. Z. Bathaie and Z. M. Hassan, *Ultrason Sonochem*, 2011, **18**, 1165-1171.
148. G. A. Husseini, N. Y. Rapoport, D. A. Christensen, J. D. Pruitt and W. G. Pitt, *Coll Surf B: Biointerfaces*, 2002, **24**, 253-264.
149. G. A. Husseini, M. A. D. de la Rosa, E. O. AlAqqad, S. Al Mamary, Y. Kadimati, A. Al Baik and W. G. Pitt, *J Franklin I*, 2011, **348**, 125-133.
150. D. Stevenson-Abouelnasr, G. A. Husseini and W. G. Pitt, *Colloid Surface B*, 2007, **55**, 59-66.
151. G. A. Husseini, W. G. Pitt, D. A. Christensen and D. J. Dickinson, *Journal of Controlled Release*, 2009, **138**, 45-48.
152. G. A. Husseini, D. Stevenson-Abouelnasr, W. G. Pitt, K. T. Assaleh, L. O. Farahat and J. Fahadi, *Colloid Surface A*, 2010, **359**, 18-24.
153. F. S. Mjalli and N. M. Abdel-Jabbar, *Ind Eng Chem Res*, 2005, **44**, 2125-2133.
154. J. Saintdonat, N. Bhat and T. J. Mcavoy, *Int J Control*, 1991, **54**, 1453-1468.
155. G. A. Husseini, F. S. Mjalli, W. G. Pitt and N. M. Abdel-Jabbar, *Technol Cancer Res T*, 2009, **8**, 479-488.
156. G. A. Husseini, N. M. Abdel-Jabbar, F. S. Mjalli and W. G. Pitt, *Technol Cancer Res T*, 2007, **6**, 49-56.
157. J. Wang, M. Pelletier, H. J. Zhang, H. S. Xia and Y. Zhao, *Langmuir*, 2009, **25**, 13201-13205.
158. A. Marin, H. Sun, G. A. Husseini, W. G. Pitt, D. A. Christensen and N. Y. Rapoport, *J. Controlled Rel.*, 2002, **84**, 39-47.
159. G. A. Husseini and W. G. Pitt, *J Nanosci Nanotechno*, 2008, **8**, 2205-2215.
160. K. Tachibana, T. Uchida, K. Tamura, H. Eguchi, N. Yamashita and K. Ogawa, *Cancer Lett.*, 2000, **149**, 189-194.

161. K. Tachibana, T. Uchida, K. Ogawa, N. yamashita and K. Tamura, *Lancet*, 1999, **353**, 1409.
162. Y. Zhou, R. E. Kumon, J. Cui and C. X. Deng, *Ultrasound in Medicine and Biology*, 2009, **35**, 1756-1760
163. A. van Wamel, K. Kooiman, M. Harteveld, M. Emmer, F. J. ten Cate, M. Versluis and N. de Jong, *Journal of Controlled Release*, 2006, **112**, 149-155.
164. R. K. Schlicher, J. D. Hutcheson, H. Radhakrishna, R. P. Apkarian and M. R. Prausnitz, *Ultrasound in Medicine and Biology*, 2010, **36**, 677-692.
165. P. Loverock, G. Ter Haar, M. G. Ormerod and P. R. Imrie, *Brit. J. Radiol.*, 1990, **63**, 542-546.
166. B. J. Staples, B. L. Roeder, G. A. Husseini, O. Badamjav, G. B. Schaalje and W. G. Pitt, *Cancer Chemother Pharmacol*, 2009, **64**, 593-600.
167. B. J. Staples, W. G. Pitt, B. Schaalje and B. L. Roeder, Controlled Release Society, Long Beach, CA, 2007.
168. J. L. Nelson, B. L. Roeder, J. C. Carmen, F. Roloff and W. G. Pitt, *Cancer Res.*, 2002, **62**, 7280-7283.
169. B. J. Staples, W. G. Pitt, B. L. Roeder, G. A. Husseini, D. Rajeev and G. B. Schaalje, *J. Pharm. Sci.*, 2010, **99**, 3122-3131.
170. N. Y. Rapoport, D. A. Christensen, H. D. Fain, L. Barrows and Z. Gao, *Ultrasonics*, 2004, **42**, 943-950.
171. S. Samuel, M. A. Cooper, J. L. Bull, J. B. Fowkes and D. L. Miller, *Ultrasound in Medicine and Biology*, 2009, **35**, 1574-1586.
172. C. Y. Lin, T. M. Liu, C. Y. Chen, Y. L. Huang, W. K. Huang, C. K. Sun, F. H. Chang and W. L. Lin, *Journal of controlled release : official journal of the Controlled Release Society*, 2010, **146**, 291-298.
173. B. D. Meijering, L. J. Juffermans, A. van Wamel, R. H. Henning, I. S. Zuhorn, M. Emmer, A. M. Versteilen, W. J. Paulus, W. H. van Gilst, K. Kooiman, N. de Jong, R. J. Musters, L. E. Deelman and O. Kamp, *Circ Res*, 2009, **104**, 679-687.
174. J. Hauser, M. Ellisman, H. U. Steinau, E. Stefan, M. Dudda and M. Hauser, *Ultrasound in medicine & biology*, 2009, **35**, 2084-2092.
175. G. A. Husseini, C. M. Runyan and W. G. Pitt, *Bmc Cancer*, 2002, **2**, 1-6.
176. S. B. Stringham, M. A. Viskovska, E. S. Richardson, S. Ohmine, G. A. Husseini, B. K. Murray and W. G. Pitt, *Ultrasound in Medicine and Biology*, 2009, **35**, 409-415.
177. D. W. Fairbairn, P. L. Olive and K. L. O'Neill, *Mutation Res.*, 1995, **339**, 37-59.
178. G. A. Husseini, K. L. O'Neill and W. G. Pitt, *Technol Cancer Res T*, 2005, **4**, 707-711.
179. A. Kheirolomoom, P. A. Dayton, A. F. H. Lum, E. Little, E. E. Paoli, H. Zheng and K. W. Ferrara, *Journal of Controlled Release*, 2007, **118**, 275-284.
180. A. L. Klibanov, T. I. Shevchenko, B. I. Raju, R. Seip and C. T. Chin, *Journal of Controlled Release*, 2010, **148**, 13-17.
181. K. Shiraishi, R. Endoh, H. Furuhata, M. Nishihara, R. Suzuki, K. Maruyama, Y. Oda, J.-i. Jo, Y. Tabata, J. Yamamoto and M. Yokoyama, *Int J Pharm*, 2012, **in press**.
182. N. Y. Rapoport, A. M. Kennedy, J. E. Shea, C. L. Scaife and K. H. Nam, *Journal of Controlled Release*, 2009, **138**, 268-276.

Figures

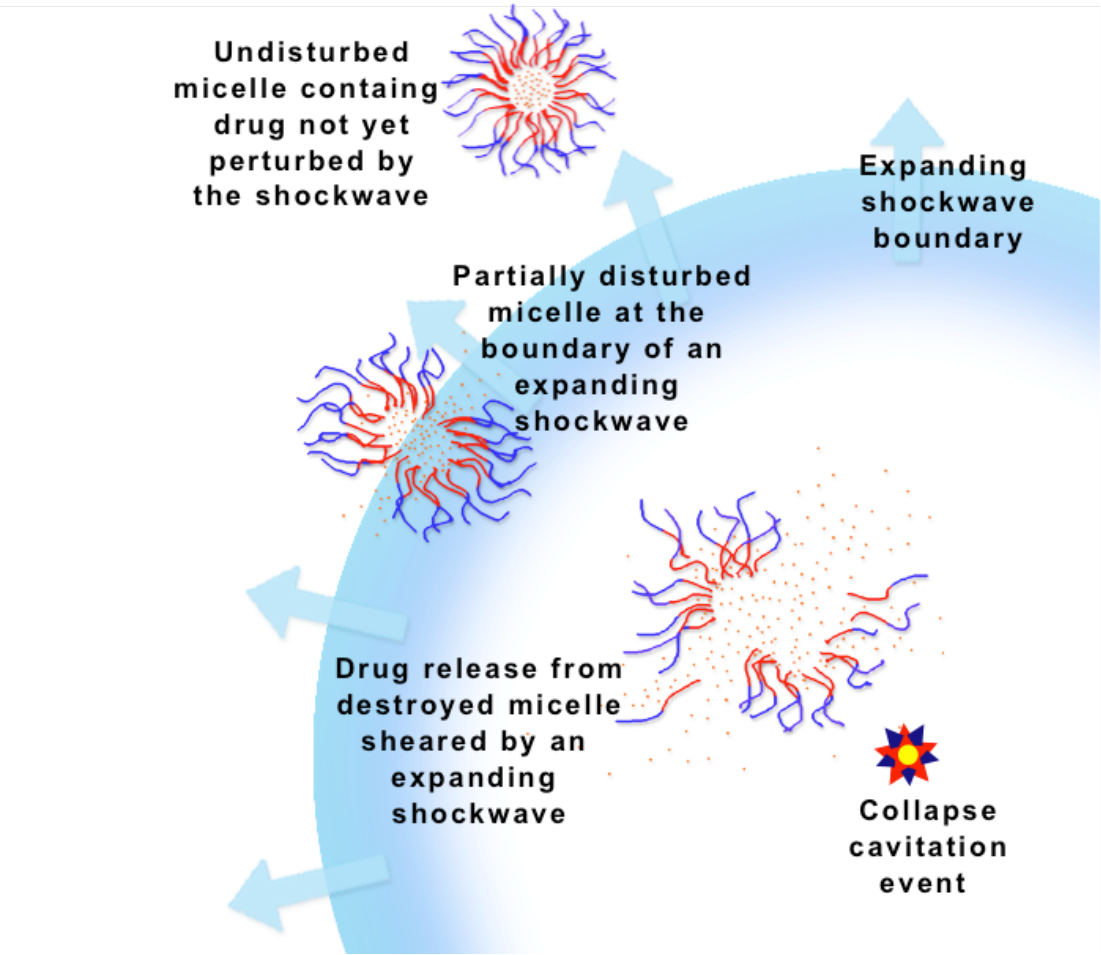

Figure 1. Illustration of an expanding shockwave from a collapse cavitation event that causes mechanical disruption of micelles. The compressional shock wave is thought to transiently shear open micelles, thus releasing their contents.

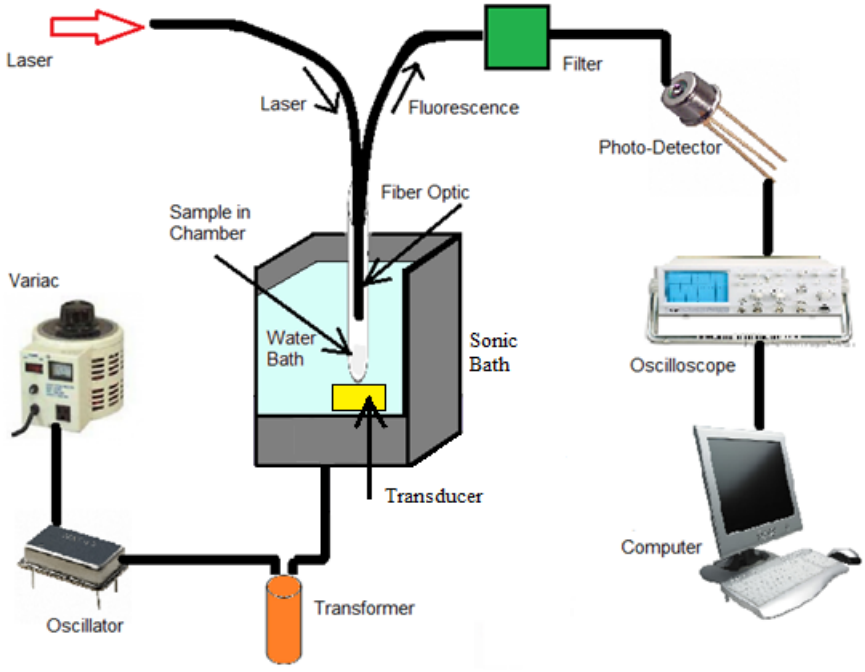

Figure 2: Fluorescence detection system with ultrasonic exposure. The intensity of ultrasound in the sonic bath is controlled by the AC voltage from a variac through an oscillator circuit and matching network (transformer). The sample is placed in an acoustically transparent plastic tube in an acoustically intense spot over the transducer. An argon ion laser beam (488 nm) is directed through a fiber optic cable into the sample chamber. The drug fluorescence is collected by a second fiber optic bundle and directed through a 533-nm band pass filter to a silicon photo-detector. The detector signal is observed with an oscilloscope and then digitized with an A/D converter and stored to a computer for post-processing conversion to released drug concentration.

Figure Captions

Figure 1. Illustration of an expanding shockwave from a collapse cavitation event that causes mechanical disruption of micelles. The compressional shock wave is thought to transiently shear open micelles, thus releasing their contents.

Figure 2: Fluorescence detection system with ultrasonic exposure. The intensity of ultrasound in the sonic bath is controlled by the AC voltage from a variac through an oscillator circuit and matching network (transformer). The sample is placed in an acoustically transparent plastic tube in an acoustically intense spot over the transducer. An argon ion laser beam (488 nm) is directed through a fiber optic cable into the sample chamber. The drug fluorescence is collected by a second fiber optic bundle and directed through a 533-nm band pass filter to a silicon photo-detector. The detector signal is observed with an oscilloscope and then digitized with an A/D converter and stored to a computer for post-processing conversion to released drug concentration.